ACCURATE DETERMINATION OF THE RELATIVE DENSITY OF SLM ADDITIVELY MANUFACTURED PARTS

C.P. Kloppers[1*] & D.J. de Beer[2]

ARTICLE INFO

Article details
Submitted by authors 17 May 2024
Accepted for publication 5 Nov 2024
Available online 13 Dec 2024

Contact details
* Corresponding author
cp.kloppers@nwu.ac.za

Author affiliations
1 School of Mechanical Engineering, North-West University, Potchefstroom, South Africa

2 NRF SARChI in Medical Product Development through AM, Central University of Technology, Bloemfontein, Free State.

ORCID® identifiers
C.P. Kloppers
https://orcid.org/0000-0001-5942-0251

D.J. de Beer
http://orcid.org/0000-0003-0175-9556

DOI
http://dx.doi.org//10.7166/35-4-3040

ABSTRACT

Additive manufacturing (AM) is a disruptive technology that provides design freedom, fast turnaround times, and a digital workflow. However, reliable mechanical and material properties are crucial for medical implants and devices produced by AM. The laser powder bed fusion (LPBF) echnique is a reliable method for producing high-quality parts with excellent mechanical properties. The presence of internal porosity, however, is one of the most significant problems in SLM part production. This study aimed to determine the relative density of components produced by LPBF and to develop a method for accurately quantifying the relative density. Three powders were used to evaluate the efficacy of three different quantification methods. The OR-Laser Creator LPBF unit was used to manufacture them. After production, all nine samples were polished on a lathe, and the relative density was measured using three different quantification methods. The results of this study showed that the Archimedes principle is the most accurate and reliable method for determining the density of materials used in LPBF. The findings of this study should help to ensure that the quality of parts produced by SLM is reliable and accurate. This should increase confidence in the use of LPBF in the medical industry and other industries where AM components have a significant advantage.

OPSOMMING

Laag vervaardiging (LV) is 'n ontwrigtende tegnologie wat ontwerpvryheid, vinnige omkeertye en 'n digitale werkvloei bied. Betroubare meganiese en materiaal eienskappe is egter deurslaggewend vir mediese inplantings en toestelle wat deur LV vervaardig word. Die laser poeier bed smelting (LPBS) tegniek is 'n betroubare metode vir die vervaardiging van hoë kwaliteit onderdele met uitstekende meganiese eienskappe. Die teenwoordigheid van interne porositeit is egter een van die belangrikste probleme in LPBS-deelproduksie. Hierdie studie het ten doel gehad om die relatiewe digtheid van komponente wat deur LPBS vervaardig word te bepaal en om 'n metode te ontwikkel om die relatiewe digtheid akkuraat te kwantifiseer. Drie LPBS-poeiers is gebruik om die doeltreffendheid van drie verskillende kwantifiseringsmetodes van porositeitsanalise te evalueer. Alle monsters het voldoen aan die ASTM F75-vereistes vir chirurgiese inplantings, en die OR-Laser Creator LPBS-eenheid is gebruik om dit te vervaardig. Na produksie is al nege monsters op 'n draaibank gepoleer, en die relatiewe digtheid is gemeet met behulp van drie verskillende kwantifiseringsmetodes. Die resultate van hierdie studie het getoon dat die Archimedes-beginsel die mees akkurate en betroubare metode is vir die bepaling van die digtheid van materiale wat in LPBS gebruik word. Die bevindinge van hierdie studie behoort te help om te verseker dat die kwaliteit van onderdele wat deur LPBS vervaardig word betroubaar en akkuraat is. Dit behoort vertroue in die gebruik van LPBS in die mediese industrie en ander nywerhede te verhoog waar AM-komponente 'n beduidende voordeel.

1. INTRODUCTION

Additive manufacturing (AM) is a field that can result in a paradigm shift in the design and manufacturing of components [1]. Advantages such as design freedom, fast turnaround times, and the digital workflow used in AM establish this as a disruptive technology in the industry [2]. Selective laser melting is an AM technique that can produce medical implants and medical devices from various materials [3,4]. Reliable mechanical and material properties ensure the service life of medical implants and medical devices produced by AM; thus it is essential to find reliable quantification methods.

Quality management systems, such as ISO 13485:2016, were established by international organisations such as the International Organization for Standardization (ISO) to provide manufacturing quality control in producing SLM parts. However, other fundamental tests can also assist producers in ensuring the quality of the part produced by SLM [5] To this end, parameters such as surface roughness, microstructure, tensile strength, inherent strain, and porosity are quantified to ensure no internal flaws in the parts produced by SLM [6]. Considering these parameters during the production processes is vital, as the porosity in parts could lead to fatigue failure owing to crack initiation locations, depending on the size and shape of the porosity [7,8]. Porosity can also lead to premature failure under loading owing to the reduced surface area distributing the load [9].

The AM community considers porosity in a part one of the most significant hurdles in SLM part production [10]. Porosity caused by insufficient energy input or by lack of fusion defects from excessive energy will result in internal porosity that has a negative impact on the mechanical properties of the components [11]. Gas pores trapped inside the manufactured parts and keyhole porosity have been studied to understand the causes behind the formation of these porosities [12,13]. Despite SLM's benefits to the various industries in which AM components have a significant advantage in their lightweight and patient-specific geometries, they cannot afford having components fail because of internal porosity [14]. Regardless of the type of porosity present in a part, measuring the percentage of porosity that is present leads to a better understanding of the quality of the produced part. This quantification is achieved by comparing the densities of the part with and without porosity being present.

Selective laser melting (SLM) is a robust additive manufacturing process that produces high-quality parts with excellent mechanical properties. The quality of the parts produced by SLM is evaluated based on the relative density of the part and the amount of porosity present in the SLM component. While SLM typically produces parts with a relative density of 99% or higher, accurately determining the relative part density becomes more difficult as the quality of the components improves. It is crucial to use reliable and accurate measurement techniques to ensure the accuracy and repeatability of the process of determining the relative part density [15]. The Archimedes principle is the most accurate and reliable method for determining the density of materials used in AM, including SLM. However, the reference values for the relative part densities are not always entirely accurate, which could lead to errors in the process.

For this reason, this study aimed to develop a method for determining the relative part density of components produced by SLM. Three different quantification methods of porosity analysis were investigated on three different SLM powders to evaluate the efficacy of the methods used to quantify the relative density.

2. MATERIALS AND METHODS

This study aimed to determine the relative density of additively manufactured parts. The study's experiments were conducted in controlled environments in the laboratory facilities at North-West University's (NWU) School of Mechanical Engineering, South Africa, unless stated otherwise because the required equipment was unavailable at NWU.

Samples were produced in the SLM unit from a metallic CoCrMo powder; three powders from three different powder manufacturers were used, and three samples per powder were produced to ensure repeatability. In all cases, the powders adhered to the ASTM F75 requirements for surgical implants. The particle size distribution was 10-45 µm for all powders, and the gas atomisation manufacturing process was used to manufacture all the powders. The SLM unit used in this study was the OR-Laser Creator, with a build size of 100 mm in diameter and a total z-axis height of 110 mm. This unit is equipped with a 250 W fibre laser, having a minimum spot size of 40 µm. Laser power for the hatching was set to 125 W with contouring set to 140 W, while laser mark speeds of 630 mm/s and 250 mm/s were used for the hatching and contouring

phase. During hatching, a 50 % overlap was used with a 120 µm laser spot size. A 40 µm spot size was used for contouring with an 80 µm boundary offset.

The material parameters used in this study and presented here were provided by the original equipment manufacturer for use in this LPBF unit with this specific material. Optimisation of volumetric energy density was not conducted before this study was executed in order to ensure that there was significant porosity in the parts that were produced and to ensure accurate quantification of the density prior to and after the densification processes.

After production of the samples, all nine were polished on a lathe using a wet polishing technique with abrasion media of up to 2000 grit. A mirror-like surface finish was obtained to ensure that the entrapment of air bubbles was limited to the absolute minimum during the Archimedes testing.

The nine samples that were produced were subjected to a non-destructive test to quantify their density in three different ways. After polishing, the Archimedes density tests were carried out to obtain the part density of the as-built samples. The samples were also subjected to micro-CT scanning to visualise the porosity in the as-built parts. Micro-CT scanning also accurately determined the total volume of the parts, and could quantify the size and shape of the internal porosity. Inductively coupled plasma optical emission spectroscopy (ICP-OES) was carried out on the powders from which the samples had been manufactured in order to gain an understanding of the elements that were present and the weight percentages in each powder. Once these quantification processes had been completed, the samples were subjected to hot isostatic pressing (HIP) to solidify the parts internally and to eliminate all porosity. All the non-destructive testing carried out pre-HIP was repeated post-HIP, except for the ICP-OES. This led to an accurate measure of the reduction in porosity.

Studies conducted by Le Bourdais *et al.* (2022) and De Terris *et al.* (2019) proved that the Archimedes method is effective in establishing baseline densities of the parts produced on the additive manufacturing unit. The Archimedes method enabled the calculation of the mean density of any complexly shaped part, incorporating the entire volume of the part and not only specific cross-sections. The part density r_p is thus given as

$$r_p = \frac{m_a}{m_a - m_f} r_f$$

with r_p denoting the fluid density and m_a and m_f respectively representing the mass of the part weighed in air and in the fluid. Each of the nine samples was weighed five times to ensure repeatability and so that a standard deviation could be calculated. This method was carried out by first weighing the samples in the air on the Adam Lab 254i Luna analytical lab balance (accurate to 0.0001 g). This was done in a temperature-controlled room set to 22 oC for a minimum of 12 hours before testing. The airflow in the room was also controlled to ensure that errant gusts of wind would not affect the results. A density kit procured for the Adam Lab 254i lab balance weighed the nine samples in 99.9% pure acetone to obtain the second weight required for the Archimedes method density calculations. Acetone was used as a working fluid rather than water because of acetone's lower surface tension and known density over a wide range of temperatures. The Archimedes method was selected based on the results obtained by Spierings et al. [15] and on their work on the density of additive manufacturing parts.

Micro-CT scanning made porosity visualisation and volume determination of all nine samples possible, as in the cases of De Chiffre et al. [16] and Kruth et al. [17]. Micro-CT scanning was carried out by X-Sight X-ray services in Somerset West, South Africa. A Nikon Metrology XTH225ST was used with 200 kV X-ray intensity and a 1 mm Cu filter, a voxel size of 0.02007 mm was obtained, and 2000 projections were carried out per scan. Micro-CT was used for both the visualisation of porosity and the accurate measurement of the sample volumes, based on the work of Du Plessis et al. [18, 19].

The nine samples were subjected to HIP to solidify the part internally and to ensure zero porosity, as established by Ng et al. [20]. Metal Heart Additive Manufacturing carried out HIP in Randburg, South Africa. The HIP was carried out in an EPSI HIP unit with a maximum temperature of 1200 oC, at a pressure of 1 MPa in an Argon gas environment, with the dwell time set to two hours. After the HIP process, the Archimedes method was carried out again on the nine samples to determine the new density of the parts. Micro-CT scanning was repeated to ensure the elimination of porosity and to determine the volume of the parts post-HIP.

ICP-OES was also performed on the material to determine each powder's chemical composition and to calculate the parts' theoretical true density [21]). ICP-OES was shown by Rodríguez-González et al. [22] to be the correct and most accurate method of determining the chemical composition of metal powders used in additive manufacturing. ICP-OES was conducted at the Pelindaba Analytical Laboratory, part of the South African Nuclear Energy Corporation (NECSA) in Pretoria, South Africa. All calculations and statistical work were processed in Microsoft Excel.

3. RESULTS

The study aimed to determine the relative density of the parts produced by selective laser melting. The reference value to which the actual part density was compared was crucial in determining the correct relative part density; a faulty input could lead to parts failing prematurely owing to porosity-induced cracking and stress concentrations. Archimedes and micro-CT scanning were used to determine a baseline density, and HIP was used to densify the parts fully. The same testing procedure was followed post-HIP treatment to obtain the reference density. ICP-OES was regarded as an alternative in order to determine the reference density values. The chemical composition of the feedstock material and the elemental weights were used to determine whether these results were comparable to those obtained from the HIP.

The results from the various tests are presented below. First the sample preparation is shown, and then the density quantification is presented. Given the nature of the manufacturing process, a rough surface finish was obtained. A lathe was used to sand down the parts to minimise the chance of air bubbles being trapped on the part surface, and progressively finer wet-sanding abrasion media were used up to 2000 grit to finish the parts. The difference can be seen in the image in Figure 1.

Figure 1: Sample (on the left) before and (on the right) after surface finishing

Table 1 shows the results of the pre-HIP samples in air and in acetone:

Table 1: Archimedes result in pre-HIP

		Average weight in air [g]	Standard deviation	Average weight in acetone [g]	Standard deviation	Part density [kg/m3]	Standard deviation
Powder 1	Sample A	8,588	0,0002	7,795	0,0002	8521,5	3,4
	Sample B	8,554	0,0002	7,766	0,0002	8540,1	3,1
	Sample C	8,394	0,0001	7,621	0,0001	8548,7	2,3
Powder 2	Sample A	8,123	0,0002	7,355	0,0004	8333,2	5,9
	Sample B	7,917	0,0001	7,167	0,0004	8323,5	3,4
	Sample C	8,146	0,0001	7,376	0,0003	8330,0	3,8
Powder 3	Sample A	8,212	0,0001	7,425	0,0002	8223,0	1,8
	Sample B	7,997	0,0001	7,230	0,0003	8209,8	3,0
	Sample C	8,081	0,0001	7,305	0,0003	8212,4	3,7

Table 1 shows the three distinct groups of powders yielding significantly different densities. Powder 1 has a significantly higher density than the other two more closely grouped powders. Powder 1 has a variation

of 0.319% difference between the three samples. Although a good result, Powder 2 and Powder 3 have variations of only 0.116% and 0.160% respectively. Although conforming to the ASTM-F75 prescription of elemental analysis for medical implants, the three powders have significant variations in elemental constituents. Thus comparing the three powders relative to one another would yield no significant results as all parts that were produced would, in all likelihood, contain a significant number of porosities. The close grouping of less than one-third of a percentage point and a low standard deviation shows the repeatability and precision of this method.

Although the specific densities of all nine samples are known, the relative part density is lacking, and the porosity in the parts is unknown. Yu *et al.* [23] and other sources stated that the density of CoCrMo is 9400 kg/m^3, implying that the relative density achieved by powder A is greater than 100% [23]. As an example, Powder 1 Sample B has a relative density of 101.667% when dividing 8540.1 kg/m^3 by the reference value of Yu *et al.* This necessitates accurate and alloy-specific reference values to quantify relative densities accurately. As cited, Ng *et al.* [20] determined that post-HIP samples contained no porosity owing to the HIP process's high-temperature and high-pressure environment. After the HIP had been carried out, the same procedure was repeated, and the results are presented in Table 2.

Table 2: Archimedes result in post-HIP

		Average weight in air [g]	Standard deviation	Average weight in acetone [g]	Standard deviation	Part density [kg/m^3]	Standard deviation
Powder 1	Sample A	8,573	0,0001	7,791	0,0001	8634,4	2,6
	Sample B	8,544	0,0001	7,764	0,0003	8625,2	2,7
	Sample C	8,380	0,0001	7,617	0,0003	8637,0	3,2
Powder 2	Sample A	8,114	0,0000	7,353	0,0004	8405,3	4,4
	Sample B	7,907	0,0001	7,166	0,0001	8405,4	0,9
	Sample C	8,133	0,0001	7,370	0,0001	8400,4	2,6
Powder 3	Sample A	8,207	0,0001	7,433	0,0002	8355,1	2,7
	Sample B	7,993	0,0000	7,238	0,0002	8344,3	2,6
	Sample C	8,077	0,0001	7,314	0,0002	8344,0	2,5

Significant densification occurred during the HIP process, with Powder 1, Powder 2, and Powder 3 having respective average densities of 1.12%, 0.90%, and 1.62% higher than before the HIP. This implies that the most porosity was present in Powder 3 and the least in Powder 2. Small standard deviation values and close grouping within the respective powders show repeatable results, with Powder 2 showing only a 0.059% variation in density across the three samples. Table 3 shows a detailed comparison of the densification during the HIP procedure.

Table 3: Densification quantification

		Weight variation - air [g]	Weight variation - acetone [g]	Change in part density [kg/m^3]	Relative part density [%]
Powder 1	Sample A	-0,015	-0,0037	112,913	98,6923
	Sample B	-0,010	-0,0017	85,039	99,0141
	Sample C	-0,014	-0,0045	88,260	98,9781
Powder 2	Sample A	-0,009	-0,0019	72,049	99,1428
	Sample B	-0,010	-0,0016	81,885	99,0258
	Sample C	-0,013	-0,0052	70,397	99,1620
Powder 3	Sample A	-0,005	-0,0079	132,114	98,4188
	Sample B	-0,004	-0,0083	134,532	98,3877
	Sample C	-0,004	-0,0086	131,555	98,4234

Densification in the HIP process for Powder 1 had a significant variation, with one sample densifying up to 30% more than the other samples of the same powder. The significant variation could be attributed to the variations in the SLM manufacturing method, with many parameters that could have caused this significant porosity in the sample. The location of the sample on the printing surface relative to the re-coater movement, the angle of the laser relative to the other samples, and the laser speed and hatching angle could have significantly influenced the porosity present in the samples. The grouping of Powder 2 and Powder 3 was significantly closer, with Sample B of Powder 2 densifying only 14.97% more than the other samples of the same powder. Although this was about half of the value of Sample A of Powder 1, this was still a significant difference.

All samples were slightly lighter because of the sanding procedure post-HIP to obtain a good surface finish and to remove the oxide layer on the parts. As expected, Powder 2 had the highest relative density: on average, 99.1102% for the specific laser parameters used. Powder 1 had a relative part density of 98.8948%, almost half a per cent higher than Powder 3, which had an average relative part density of 98.4099%. The relative part densities were within the expected range for the selected laser melting manufacturing process. Powders 1 and 3 were below 99% relative part density, which could be improved by altering the laser energy density during manufacturing.

The relative part densities achieved by the SLM unit were somewhat low compared with what could be expected from SLM units with optimised printing parameters for laser energy density. The location size and shape of these densities could lead to insights into effectively improving the printing parameters of the SLM unit used in this study.

The visualisation of porosities and quantifying of size and shape were achieved by micro-CT scanning. Micro-CT scanning is a means of visualising the porosity and obtaining a measurement of the volume of each sample. As the micro-CT scanning can accurately quantify the variations in density, the outer surface of the sample can also be accurately determined. In turn, the volume can be calculated. The visualisation of porosities is not without limitations. The parameters mentioned in the section above indicated a voxel size of 20 µm for these samples. Thus no porosity below the size of the voxel is visualised in the images presented below.

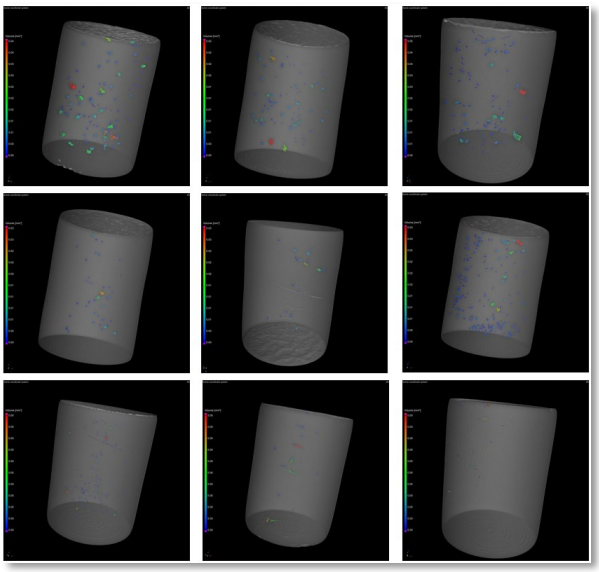

Figure 2: Porosity visualisation using micro-CT scanning

It is clear from the images in Figure 2 that the significant number of large porosities in Sample A of Powder 1, with 12 pours larger than 300 µm, was consistent with the results obtained from the Archimedes testing and the densification experienced during the HIP. Sample B of Powder 2 does not look worse visually than the other samples from the same powder, even with Sample C registering more fine porosities. This may be because many fine porosities under the minimum voxel size of 20 µm cannot be visualised.

Based on visual results, Powder 3 performed best with the least porosity visible, with Sample B and Sample C registering only 16 and 19 porosities respectively. Although this is the case visually, the reality is alluded to in the results of Sample C, with all the porosity being smaller than 150 µm. The most likely case is that Powder 3 contained many porosities smaller than the minimum voxel size. The density results yielded from the micro-CT scanning were contradictory to the results obtained from the Archimedes method, with Powder A having an average density of 9006.13 kg/m^3, and Powder 2 and Powder 3 with 8785.5 kg/m^3 and 8641.2 kg/m^3 respectively. This density calculation was based on a volume measurement conducted during the micro-CT scanning process, and this measurement was once again based on the voxel resolution of the object being scanned. This could have had a significant impact on the accuracy of the result, as can be seen.

Table 4: Micro-CT porosity count

		Sample volume [mm^3]	Sample weight in air [g]	Sample density [kg/m^3]	Number of porosities	Number of porosities larger than 300mm	Number of porosities between 300m and 150mm	Number of porosities smaller than 150mm
Powder 1	Sample A	953,73	8,588	9004,8	89	12	61	16
	Sample B	953,82	8,554	8968,4	82	3	38	41
	Sample C	927,99	8,394	9045,2	95	3	41	51
Powder 2	Sample A	928,18	8,123	8751,9	38	1	23	14
	Sample B	903,82	7,917	8759,3	38	1	11	26
	Sample C	927,22	8,146	8785,5	168	4	93	71
Powder 3	Sample A	952,10	8,212	8625,0	99	0	3	96
	Sample B	928,56	7,997	8612,5	16	0	5	11
	Sample C	930,31	8,081	8686,0	19	0	0	19

The final alternative method to determine relative part density is an approximation using the material's chemical composition and the elemental weights. The results in Table 4 show that, for each powder, the ICP-OES results do not add to 100%. Powder 1 adds up to 99.45% when all the weight contributions are added. Powders 2 and 3 perform even worse, with 99.35% and 99.31% respectively. With typical parts produced by selective laser melting being 99% or more dense, the 0.6% to 0.7% fault margin would significantly impact the reference values when calculating the relative part density.

Table 5: ICP-OES results

	Powder 1 weight %	Density contribution	Powder 2 weight %	Density contribution	Powder 3 weight %	Density contribution
Aluminium	0,07	1,890	0,12	3,240	0,07	1,890
Calcium	0,08	1,240	0,1	1,550	0,08	1,240
Cobalt	65,7	5847,300	62,8	5589,200	63,4	5642,600
Chromium	27,1	1948,490	28,7	2063,530	29	2085,100
Iron	0,04	3,148	0,47	36,989	0,47	36,989
Manganese	0,01	0,743	0,15	11,145	0,29	21,247
Molybdenum	5,33	544,726	6,25	638,750	5,32	543,704
Nickel	0,04	3,560	0,25	22,250	0,11	9,790
Titanium	0,01	0,454	0,01	0,454	0,01	0,454
Silicon	1,07	24,931	0,5	11,650	0,56	13,048
Total weight %	99,45		99,35		99,31	
Calculated density [kg/m^3]		8376,5		8378,8		8356,4

The density is calculated by multiplying the elemental density of each element by the weight percentage present in the alloy; this then calculates the density contribution, and the sum of all the density contributions makes up the calculated density of the alloy. The results from the ICP-OES also indicate that the three different alloys that made up the three powders for this study should have had similar densities. The maximum variation in expected density was between Powder B and Powder C, with a 0.3% variation in expected density. Powder A and Powder B should, according to the ICP-OES results, have varied by only 0.13%, but Powder A was 3.7% more dense than Powder B. This showed the effect of the variations in the ICP-OES results and their effect on the densities of the powders.

Although manufacturing process variations significantly affected the parts' relative part density, the HIP procedure eliminated these with a very close grouping of densities post-HIP. Variations of 30.3% for Sample A of Powder 1 and 14.89% for Sample B of Powder 2 did not have a significant impact on the density post-HIP, showing the effectiveness of this procedure. It is also noted that there can be significant variations of parts produced in the same manner, with only a few millimetres in placement variation on the build plate. This would necessitate the measurement of density (Archimedes or micro-CT scanning) of all parts after the manufacturing process, as there are no visible differences to the naked eye.

The method of determining the relative part density with both micro-CT and ICP-OES has inherent flaws, limiting their accuracy in determining the reference value for calculating the relative part density. Micro-CT scanning, although the most expensive alternative, has a limitation of voxel size and is effectively blind below the voxel size of 20 µm in this case. ICP-OES is a good approximation of the chemical composition of the powders, but has an inherent limitation.

Variances in part density imply the formation of porosities during the manufacturing process; this could lead to premature part failure and, even more so, to failure under cyclic loading of the parts. Accurate quantification of relative part densities is essential to ensure trust in the part's performance during its service life. For this study, relative part density could be best quantified using the HIP procedure and the Archimedes method. A summary of the density quantification is included in Table 6.

Table 6: Density Comparison

		Pre-HIP Archimedes [kg/m^3]	**Post-HIP Archimedes [kg/m^3]**	**Pre-HIP micro-CT [kg/m^3]**
Powder 1	Sample A	8521.5	8634.4	9004.8
	Sample B	8540.1	8625.2	8968.4
	Sample C	8548.7	8637.0	9045.2
Powder 2	Sample A	8333.2	8405.3	8751.9
	Sample B	8323.5	8405.4	8759.3
	Sample C	8330.0	8400.4	8785.5
Powder 3	Sample A	8223.0	8355.1	8625.0
	Sample B	8209.8	8344.3	8612.5
	Sample C	8212.4	8344.0	8686.0

4. CONCLUSION

The focus of this paper was to develop a method to determine accurately the relative part density of parts manufactured by SLM. Relative part density quantifies the quality of the parts produced in an SLM process. When quantifying relative part density, an understanding of the porosity inside the part is obtained. In turn, process parameters such as laser power, hatching speed, layer thickness, and laser spot size can be manipulated to obtain more dense parts. The density of a part produced by SLM must be compared with a reference value to determine the relative part density. Obtaining this reference value is just as important as accurately determining the density of the part.

Three different powders were used, and three different samples of each powder were manufactured to test the repeatability of the quantification methods. Three different approaches were used with each of the nine samples to determine the most accurate manner of determining relative part density. An ICP-OES

analysis was carried out to determine the exact chemical composition of the alloy in each case. With this known, the elemental densities could be used to determine the true solid density of the alloy. Micro-CT scanning was used to visualise the porosity of the parts and to gain an accurate measure of the part volume; with the known volume and CoCrMo bulk density used from the literature, the relative part density could be assessed. HIP was also found in the literature to densify the parts fully owing to the high temperature and pressure in the HIP process; the Archimedes principle and the pre-and post-HIP results could also be used to quantify the relative density.

The results obtained from ICP-OES only quantified the elements in the alloy accurately to between 99.31% and 99.45%. Because of the high relative densities expected from the SLM process, this would lead to inaccurate results. The densities of 8376.5 kg/m^3, 8378.8 kg/m^3 and 8356.4 kg/m^3 obtained for powders A, B, and C respectively were in line with and within 0.52% of the expected values from the literature of 8400 kg/m^3. Although these results proved to be within half a per cent of the expected values when optimising parameters to within 0.1% of relative density, this lacks accuracy.

Micro-CT scanning was used to visualise the porosity in samples produced by SLM. With this visualisation and the post-processing porosity analysis, this analysis method could quantify the porosity in the samples. With an analysis of the size and shape of the porosity and an accurate measure of the total part volume, it was possible to determine the relative part density. As in all measurement techniques, there were limitations with regard to the part and sensor sizes. The minimum voxel size that could be obtained from micro-CT scanning was 20 µm^3 Thus all porosity under this size was effectively omitted from the analysis. The results obtained, specifically from Powder C, showed that this would be a limitation. Most of the porosity present in the samples manufactured from powder C were smaller than the limitation size of this micro-CT scanner.

The use of the Archimedes principle and the HIP yielded the most effective way of quantifying the relative part density in this study. With careful preparation of the samples and the use of acetone as a working fluid, the most accurate and consistent results were obtained. The repeatability of the process produced a range of standard deviation values of less than 3 kg/m^3, which is 0.03% of the sample density. This aligns with the findings of Spierings *et al.* [15], who found it to be the most accurate and repeatable quantification method if the samples were prepared correctly. The considerable variation in the change in part density post-HIP confirmed the findings of other authors that there is significant variation in parts produced in the same environment under the same conditions, showing the lack of control over the SLM process. However, the close grouping of the post-HIP densities showed the effectiveness of this process for parts produced by SLM.

Determining the relative part densities in parts used in critical load-bearing applications is crucial to understanding their performance in service. As there are variations in production parameters when the powder is manufactured and in the feedstock material, it would be most advantageous to produce witness samples for each production batch of these mission-critical parts. Given the nature of the SLM process and the variation of placement of parts in the build area, the density quantification pre- and post-HIP should be carried out on these witness samples to ensure high-quality parts with a predictable service life.

DATA DECLARATION STATEMENT

The data is available on request from the authors.

REFERENCES

[1] **Zhang, H., Ding, X., Guo, H., Xu, S., Li, H., Nishiwaki, S., Chen, Y. & Takezawa, A.** 2023. Multiscale topology optimisation of biodegradable metal matrix composite structures for additive manufacturing. *Applied Mathematical Modelling*, 114, 799-822.

[2] **Huang, L., Yuan, H. & Zhao, H.** 2023. An FEM-based homogenisation method for orthogonal lattice metamaterials within micropolar elasticity. *International Journal of Mechanical Sciences*, 238, 107836.

[3] **Garcia-Cabezon, C., Hernández, C. G., Castro-Sastre, M. A., Fernandez-Abia, A. I., Rodriguez-Mendez, M. L. & Martin-Pedrosa, F.** 2023. Heat treatments of 17-4 PH SS processed by SLM to improve its strength and biocompatibility in biomedical applications. *Journal of Materials Research and Technology*, 26, 3524-3543.

[4] **Kardos, K., Told, R., Pentek, A., Sahai, N., Banfai, K., Vizi, A., Koltai, A., Szabo, P., Gurdan, Z., Bovari-Biri, J., Pongracz, J. E., Telek, E., Lukacs, A. & Maroti, P.** 2024. Surface disinfection change the mechanical, structural and biological properties of flexible materials used for additive manufacturing of medical devices. *Materials & Design*, 237.

[5] **Nandhakumar, R. & Venkatesan, K.** 2023. A process parameters review on selective laser melting-based additive manufacturing of single and multi-material: Microstructure, physical properties, tribological, and surface roughness. *Materials Today Communications*, 35, 1055308.

[6] **Subasic, M., Olsson, M., Dadbakhsh, S., Zhao, X., Krakhmalev, P. & Mansour, R.** 2024. Fatigue strength improvement of additively manufactured 316L stainless steel with high porosity through preloading. *International Journal of Fatigue*, 180, 108077.

[7] **Tang, M. & Pistorius, P. C.** 2017. Oxides, porosity and fatigue performance of AlSi10Mg parts produced by selective laser melting. *International Journal of Fatigue*, 94, 192-201.

[8] **Snow, Z., Nassar, A. R. & Reutzel, E. W.** 2020. Invited review article: Review of the formation and impact of flaws in powder bed fusion additive manufacturing. *Additive Manufacturing*, 36, 101457.

[9] **Liu, B., Fang, G., Lei, L. & Yan, X.** 2022. Predicting the porosity defects in selective laser melting (SLM) by molten pool geometry. *International Journal of Mechanical Sciences*, 228, 107478.

[10] **Kousoulas, P. & Guo, Y. B.** 2023. On the probabilistic prediction for extreme geometrical defects induced by laser-based powder bed fusion. *CIRP Journal of Manufacturing Science and Technology*, 41, 124-134.

[11] **Li, J., Cao, L., Xu, J., Wang, S. & Zhou, Q.** 2022. In situ porosity intelligent classification of selective laser melting based on coaxial monitoring and image processing. *Measurement*, 187, 110232.

[12] **Tan, P., Kiran, R. & Zhou, K.** 2021. Effects of sub-atmospheric pressure on keyhole dynamics and porosity in products fabricated by selective laser melting. *Journal of Manufacturing Processes*, 64, 816-827.

[13] **De Formanoir, C., Hamidi Nasab, M., Schlenger, L., Van Petegem, S., Masinelli, G., Marone, F., Salminen, A., Ganvir, A., Wasmer, K. & Logé, R. E.** 2024. Healing of keyhole porosity by means of defocused laser beam remelting: *Operando* observation by X-ray imaging and acoustic emission-based detection. *Additive Manufacturing*, 79, 103880.

[14] **Hatami, S.** 2021. Variation of fatigue strength of parts manufactured by laser powder bed fusion. *Powder Metallurgy*, 65, 259-264.

[15] **Spierings, A. B., Schneider, M. & Eggenberger, R.** 2011. Comparison of density measurement techniques for additive manufactured metallic parts. *Rapid Prototyping Journal*, 17, 380-386.

[16] **De Chiffre, L., Carmignato, S., Kruth, J. P., Schmitt, R. & Weckenmann, A.** 2014. Industrial applications of computed tomography. *CIRP Annals*, 63, 655-677.

[17] **Kruth, J. P., Bartscher, M., Carmignato, S., Schmitt, R., De Chiffre, L. & Weckenmann, A.** 2011. Computed tomography for dimensional metrology. *CIRP Annals*, 60, 821-842.

[18] **Du Plessis, A., Razavi, S. M. J., Wan, D., Berto, F., Imdaadulah, A., Beamer, C., Shipley, J. & Macdonald, E.** 2022. Fatigue performance of shelled additively manufactured parts subjected to hot isostatic pressing. *Additive Manufacturing*, 51, 102607.

[19] **Du Plessis, A., Yadroitsava, I. & Yadroitsev, I.** 2020. Effects of defects on mechanical properties in metal additive manufacturing: A review focusing on X-ray tomography insights. *Materials & Design*, 187, 108385.

[20] **Ng, C. H., Bermingham, M. J. & Dargusch, M. S.** 2023. Eliminating porosity defects, promoting equiaxed grains and improving the mechanical properties of additively manufactured Ti-22V-4Al with super-transus hot isostatic pressing. *Additive Manufacturing*, 72, 103630.

[21] **Zhang, X., Mu, Y., Lu, N., Li, Q., Chen, S., Zhou, Y., Sun, X., Liang, J. & Li, J.** 2024. Effect of solid solution elements on cracking susceptibility of Ni-based superalloys during additive manufacturing. *Journal of Materials Science & Technology*, 190, 218-228.

[22] **Rodríguez-González, P., Ruiz-Navas, E. M. & Gordo, E.** 2020. Chemical composition and mechanical properties of wires obtained by powder extrusion for additive manufacturing. *Proceedings — Euro PM2020 Congress and Exhibition, 2020*.

[23] **Yu, B., Gu, Y., Lin, J., Liu, S., Zhang, S., Kang, M., Xi, Y., Gao, Y., Zhao, H. & Ye, Q.** 2023. Surface polishing of CoCrMo alloy by magnetorheological polishing. *Surface and Coatings Technology*, 475, 130162.